Materials Science & Engineering A 614 (2014) 264–272

Contents lists available at ScienceDirect

Materials Science & Engineering A

journal homepage: www.elsevier.com/locate/msea

Estimation of surface equi-biaxial residual stress by using instrumented sharp indentation

Zhike Lu [a,b], Yihui Feng [a], Guangjian Peng [c], Rong Yang [a], Yong Huan [a], Taihua Zhang [c,*]

[a] State Key Laboratory of Nonlinear Mechanics (LNM), Institute of Mechanics, Chinese Academy of Sciences, No. 15 Beisihuanxi Road, Beijing 100190, China
[b] University of Chinese Academy of Sciences, No. 19A Yuquan Road, Beijing 100049, China
[c] College of Mechanical Engineering, Zhejiang University of Technology, No. 18 Chaowang Road, Hangzhou 310014, China

ARTICLE INFO

Article history:
Received 20 May 2014
Received in revised form
13 July 2014
Accepted 14 July 2014
Available online 22 July 2014

Keywords:
Residual stress
Instrumented indentation
Metals
Mechanical testing
Finite element analysis

ABSTRACT

Herein, we describe a method that can be used to estimate the surface equi-biaxial residual stress of a material using instrumented sharp indentation. In this method, the fractional change in the loading curvature, rather than the contact area, was chosen as the analytical parameter; this fractional change can be more precisely obtained. A linear relationship between the fractional change in the loading curvature and the normalized equi-biaxial residual stress was found via dimensional and finite element analysis, and this linear relationship greatly simplifies the formulas associated with this method. Moreover, the proposed method was successfully verified using experimental data from our laboratory and from the literature.

1. Introduction

It is important to be able to estimate the surface residual stresses that exist in metal parts and structures because they can enhance or undermine the mechanical performance (e.g., fatigue, fracture, corrosion, and wear) of these materials. Hence, various methodologies have been developed to estimate surface residual stress. These methods can be divided into two categories: mechanical methods (e.g., hole-drilling and saw-cutting) and physical methods (e.g., X-ray and neutron diffraction) [1]. Each of these methods has its intrinsic shortcomings. Instrumented indentation testing (IIT) is a newly developed technique that has many advantages over these traditional methods for estimating the surface residual stress of a material. It is non-destructive compared to other conventional mechanical methods, and it is superior to physical methods because the testing can be localized to a particular area. In IIT, indentation depths between 10^{-1} and 10^{0} μm are usually used, and spatial resolutions between 10^{0} and 10^{1} μm can be obtained. Physical methods use penetration depths between 10^{0} and 10^{5} μm and have spatial resolutions between 10^{2} and 10^{3} μm.

The effects of residual stress on the results obtained using IIT were first reported by Tsui et al. [2] and Boshakov et al. [3] in 1996. Using experimental observations and finite element analysis, they discovered three instructive phenomena: (1) Tensile residual stress tends to lower the loading curve, while compressive residual stress tends to raise it. (2) Residual stress has a minimal influence on indentation hardness (H_{IT}). (3) The contact areas of stressed and unstressed materials differ even when they are indented to the same indentation depth. Interestingly, Sakharova et al. [4] reported that there is a linear relationship between the fractional change in the indentation load ($(F-F_0)/F_0$) and the normalized residual stress (σ^R/σ_y), and that this relationship can be utilized to evaluate the residual stress of a material.

Based on these thought-provoking discoveries, researchers proposed several analytical methods that can be utilized to estimate the surface residual stress of a material using IIT. In 1998, Suresh and Giannakopouls [5] proposed a method to determine the equi-biaxial residual stress of a material using the difference in contact area between stressed and unstressed materials indented to the same depth. In 2003, Lee and Kwon [6] created a new method to estimate residual stress using the load difference between stressed and unstressed specimens at the same indentation depth. However, both of these methods require the contact area to be measured. Subsequently, Zhao et al. [7] suggested a method to determine the residual stress, elastic modulus and yield stress of a material from the load–depth curve gathered from one conical indentation test. In this method, the contact area does not need to be measured; however, 56 empirical coefficients are involved, and it is only suitable for perfectly elastic plastic materials.

Herein, we propose a novel method based on IIT that can be used to estimate the surface equi-biaxial residual stresses in metal parts and structures. The fractional change in the loading curvature

* Corresponding author. Postal address: No. 18 Chaowang Road, Hangzhou 310014, China. Tel.: +86 571 88320762.
E-mail address: zhangth@zjut.edu.cn (T. Zhang).

http://dx.doi.org/10.1016/j.msea.2014.07.041
0921-5093/

$((c-c_0)/c_0)$ was chosen as the analytical parameter because it typically reflects the effects of residual stresses on IIT outcomes and because it can be precisely obtained from the loading curves. First, a dimensionless relationship between $(c-c_0)/c_0$ and σ^R/σ_y was derived using dimensional analysis. Then, numerical simulations were performed to fit this equation by varying the values associated with residual stress and the properties of the materials. Finally, accuracy and sensitivity analyses were performed via finite element and error propagation analyses, respectively. The validity and reliability of the method were verified using experimental data both from our laboratory and from the literature [8,9].

2. Forward analysis

2.1. Model hypothesis

The mechanical model is illustrated in Fig. 1. The surface of the sample is flat over a length many times larger than the circumscribed diameter of the indentation. The sample was penetrated to a depth less than 1/10 of its thickness by a conical indenter with a half apex angle of 70.3° (equal to the equivalent semi-conical angle of Berkovich or Vickers indenters). The equi-biaxial residual stress was assumed to be uniform over the indentation depth (see Fig. 1). The material of the specimen was modeled using the elastic-power law strain hardening plastic constitutive relationship, a widely accepted approximation for most metals. The uni-axial true stress–true strain relationship can be expressed as

$$\sigma = \begin{cases} E\varepsilon, & \text{for} \quad \varepsilon \le \frac{\sigma_y}{E}, \\ E{\varepsilon_y}^{1-n}\varepsilon^n, & \text{for} \quad \varepsilon \ge \frac{\sigma_y}{E}, \end{cases} \tag{1}$$

where E is the elastic modulus, σ_y is the yield stress, n is the strain-hardening exponent, and ε_y is the ratio of the yield stress to the elastic modulus.

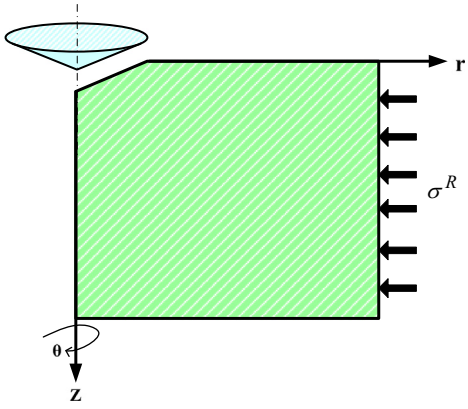

Fig. 1. A schematic showing the conical indentation of a specimen with equi-biaxial residual stress.

2.2. Dimensional analysis

For a sharp indenter penetrating a stressed specimen, the load (F) must be a function of the following seven independent parameters: the elastic modulus (E), Poisson's ratio (ν), the yield stress (σ_y), the strain hardening exponent (n) of the specimen, the equivalent half apex angle (α), the indentation depth (h), and the equi-biaxial residual stress (σ^R). In other words,

$$F = f(E, \nu, \sigma_y, n, \alpha, h, \sigma^R). \tag{2}$$

For a sharp indentation into an unstressed specimen, the load can be expressed as

$$F_0 = f_0(E, \nu, \sigma_y, n, \alpha, h), \tag{3}$$

where F_0 is the indentation load without residual stress. By applying the Π theorem in the dimensional analysis, Eqs. (2) and (3) can be rewritten as

$$F = \sigma_y h^2 f\left(\frac{E}{\sigma_y}, \nu, n, \alpha; \frac{\sigma^R}{\sigma_y}\right) = ch^2, \tag{4}$$

$$F_0 = \sigma_y h^2 f_0\left(\frac{E}{\sigma_y}, \nu, n, \alpha\right) = c_0 h^2, \tag{5}$$

where c and c_0 are the loading curvatures of the indentations with and without residual stress, respectively. Based on Eqs. (4) and (5), the ratio $(c-c_0)/c_0$ is

$$\frac{c-c_0}{c_0} = \frac{f((E/\sigma_y), \nu, n, \alpha; (\sigma^R/\sigma_y)) - f_0((E/\sigma_y), \nu, n, \alpha)}{f_0((E/\sigma_y), \nu, n, \alpha)} = g\left(\frac{E}{\sigma_y}, \nu, n, \alpha; \frac{\sigma^R}{\sigma_y}\right). \tag{6}$$

Because the functional dependence on ν is weak [10] and the equivalent half apex angle is constant (equal to 70.3°), Eq. (6) can be simplified to

$$\frac{c-c_0}{c_0} = \prod\left(\varepsilon_y, n; \frac{\sigma^R}{\sigma_y}\right). \tag{7}$$

Up to this point, the dimensionless function $\Pi(\varepsilon_y, n; \sigma^R/\sigma_y)$ has been derived to relate the indentation response to the equi-biaxial residual stress. However, this function cannot be known from the

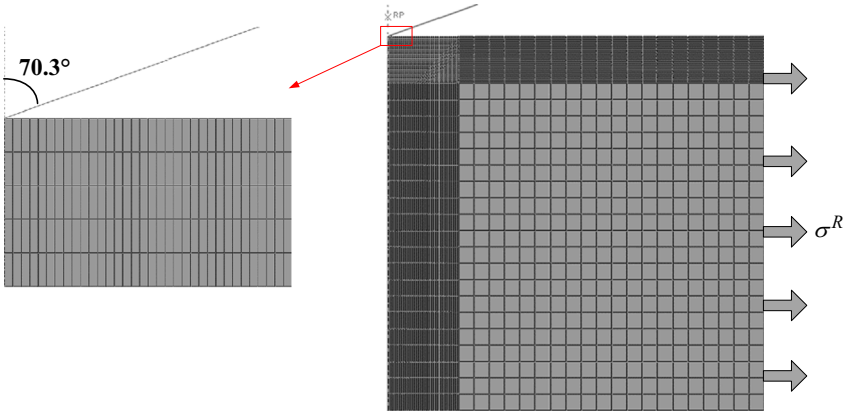

Fig. 2. The finite element mesh used in the simulation of IIT on specimens with equi-biaxial residual stress.

Table 1
The properties of the materials and the residual stresses used in the simulations. A total of 660 combinations exist.

Elastic modulus E (GPa)	Poisson's ratio ν	Yield strain $\varepsilon_y=\sigma_y/E$	Hardening exponent n	Normalized residual stress σ^R/σ_y
100	0.3	0.001	0.05	−0.9
		0.002	0.10	−0.7
		0.003	0.15	−0.5
		0.004	0.20	−0.3
		0.005	0.25	−0.1
		0.006	0.30	0
		0.007		0.1
		0.008		0.3
		0.009		0.5
		0.010		0.7
				0.9

dimensional analysis alone, and it must be obtained either experimentally or by performing simulations.

2.3. Finite element analysis

The commercially available finite element software ABAQUS [11] was used to simulate the problem of a conical rigid indenter penetrating into a semi-infinite homogeneous elastic-power law strain hardening material with equi-biaxial residual stress. Due to the symmetry of this problem, an axisymmetric model was adopted (see Fig. 2). The indenter was modeled as an analytical rigid cone with a half apex angle (α) of 70.3°, and the specimen was treated as a body of revolution that was 400 μm high with a radius of 400 μm with 3000 CAX4R elements. Roller boundary conditions were applied along the axis of symmetry and on the bottom surface of the specimen. The equi-biaxial residual stress (σ^R) was simulated by applying pressure on the outer cylindrical surface of the specimen. Coulomb's friction law was applied between the contact surfaces (with a friction coefficient of 0.15). In each simulation, the maximum indentation depth was 10 μm, and the number of the contact elements in the contact zone was greater than 40. To obtain the dimensionless function, we varied ε_y, n, and σ^R/σ_y from 0.001 to 0.010, 0.05 to 0.30, and −0.9 to 0.9 ('−' indicates compression, and the specific values are shown in Table 1), respectively. These values cover most combinations of mechanical properties and residual stresses for engineered metal materials. For convenience, we fixed the elastic modulus (E) at 100 GPa because it does not influence the dimensionless function and Poisson's ratio (ν) at 0.3 because it has only a minor effect on indentation [10].

Typical load–depth curves of indentations with different ε_y and σ^R/σ_y values are shown in Fig. 3. All of the loading curves generally agree with the forms of Eqs. (4) and (5) as predicted by dimensional analysis. The loading curves that display compressive residual stress are above those that do not display residual stress; the loading curves that display tensile residual stress are below those that do not display residual stress. When the absolute value of residual stress decreases, the loading curve tends to move towards that that does not display residual stress. In addition, when ε_y increases, the effect of the residual stress on the indentation loading curves becomes more significant.

The ratio $(c-c_0)/c_0$ was obtained by determining the indentation loading curvatures using Eqs. (4) and (5), and its relationship with the normalized residual stress (σ^R/σ_y) is illustrated in Fig. 4. The variation of $(c-c_0)/c_0$ with respect to σ^R/σ_y for materials with different ε_y and a constant strain-hardening exponent $n=0.30$ is shown in Fig. 4a. Obviously, $(c-c_0)/c_0$ has a linear relationship with σ^R/σ_y. The slope of a plot of $(c-c_0)/c_0$ vs. σ^R/σ_y not only differs for compressive and tensile residual stress, but it also decreases with increasing ε_y. Fig. 4b shows the variation in $(c-c_0)/c_0$ with

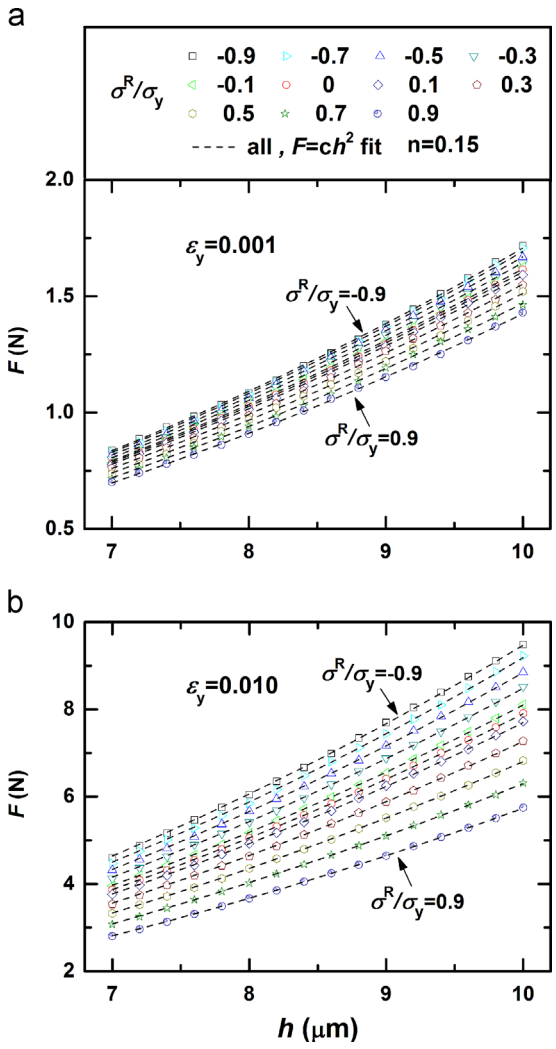

Fig. 3. The influence of residual stress on the indentation loading curves in materials with different ε_y values and a constant $n=0.15$: (a) $\varepsilon_y=0.001$; (b) $\varepsilon_y=0.010$.

respect to σ^R/σ_y for materials with different strain-hardening exponents and a constant ε_y of 0.010. These data indicate that $(c-c_0)/c_0$ varies linearly with σ^R/σ_y. Likewise, the slope of the plot of $(c-c_0)/c_0$ vs. σ^R/σ_y is asymmetric. In addition, the slope decreases with decreasing n. Because $(c-c_0)/c_0$ and σ^R/σ_y have a linear relationship as shown in Fig. 4, we can further simplify Eq. (7) to

$$\frac{c-c_0}{c_0}=f(\varepsilon_y,n)\frac{\sigma^R}{\sigma_y}, \tag{8}$$

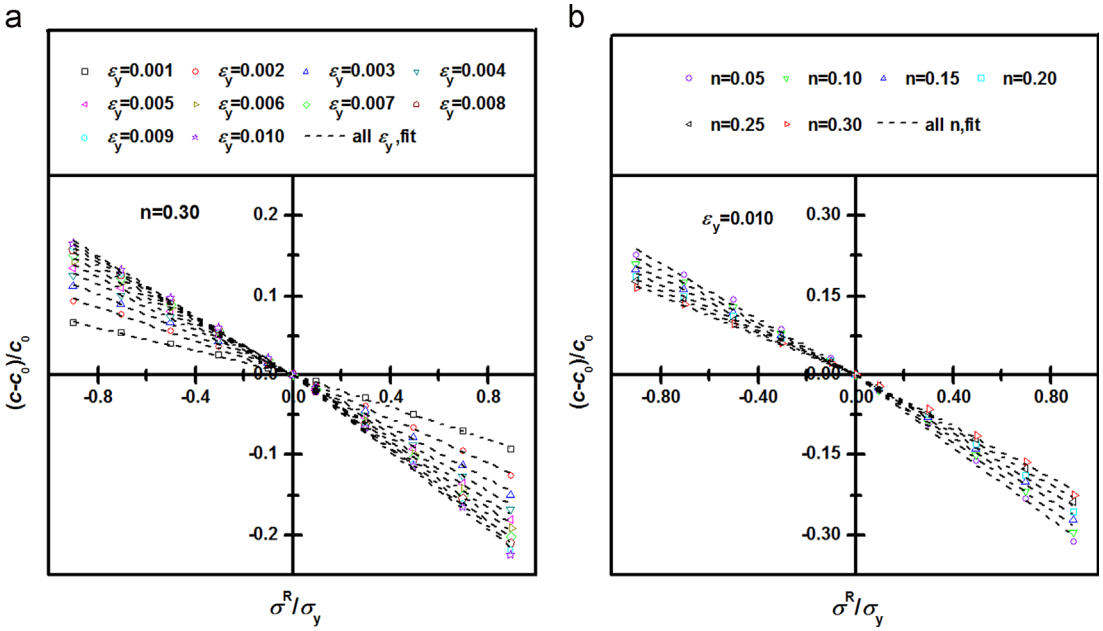

Fig. 4. The linear relationship between fractional change in loading curvature ($(c-c_0)/c_0$) and relative stress (σ^R/σ_y) in materials with different ε_y and n: (a) n=0.30; (b) ε_y=0.010. The slope is different for compressive residual stress and tensile residual stress.

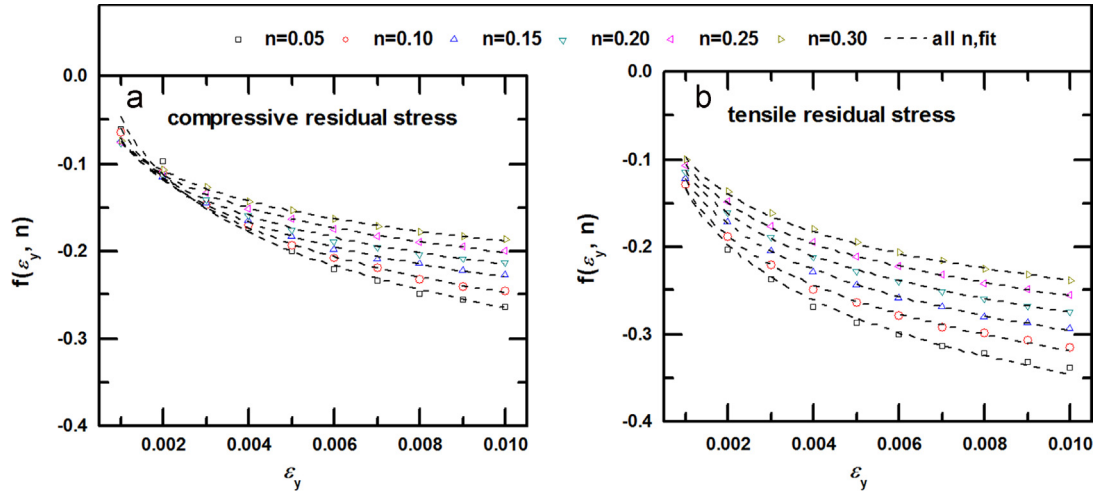

Fig. 5. The relationship between the slope function $f(\varepsilon_y, n)$ and the material properties for two cases: (a) compressive residual stress; (b) tensile residual stress. The results were calculated using Eqs. (9) and (10), respectively.

where $f(\varepsilon_y, n)$ is different for compressive residual stress and tensile residual stress and dependent upon the properties of the material.

The slope function $f(\varepsilon_y, n)$ was evaluated by fitting the linear coefficients of various materials (Fig. 5). For compressive residual stress, the function of $f(\varepsilon_y, n)$ is

$$f(\varepsilon_y, n) = (-1.0515n^2 + 0.7815n - 0.25528)\lg(\varepsilon_y) - 2.36329n^2 + 1.9639n - 0.79588, \quad (9)$$

whereas for tensile residual stress, the function of $f(\varepsilon_y, n)$ becomes

$$f(\varepsilon_y, n) = (-0.577n^2 + 0.47181n - 0.23222)\lg(\varepsilon_y) - 1.58988n^2 + 1.52078n - 0.83757. \quad (10)$$

Thus far, the analytical equation relating the indentation parameter $(c-c_0)/c_0$ to the normalized equi-biaxial residual stress (σ^R/σ_y) has been established as

$$\frac{\sigma^R}{\sigma_y} = \begin{cases} [(-1.0515n^2 + 0.7815n - 0.25528)\lg(\varepsilon_y) \\ -2.36329n^2 + 1.9639n - 0.79588]^{-1\frac{c-c_0}{c_0}} & , \quad \text{for}(c-c_0) > 0, \\ [(-0.577n^2 + 0.47181n - 0.23222)\lg(\varepsilon_y) \\ -1.58988n^2 + 1.52078n - 0.83757]^{-1\frac{c-c_0}{c_0}} & , \quad \text{for}(c-c_0) < 0. \end{cases} \quad (11)$$

3. Reverse analysis

3.1. The principle of reverse analysis

By directly applying Eq. (11) (presented in Section 2.3), we developed a new method for determining the equi-biaxial residual stress of a material (Fig. 6). After indentation tests were performed on specimens with and without residual stress, c and c_0 were calculated using Eqs. (4) and (5). If the properties of a material

have been determined by a tensile or indentation test [10,12], its equi-biaxial residual stress can be easily obtained using Eq. (11).

3.2. Accuracy analysis using finite element analysis

Numerical simulations of indentations were used to assess the accuracy of the reverse analysis for materials with different combinations of properties and residual stresses. The fractional change in the loading curvature ($(c-c_0)/c_0$) was calculated from the loading curves, and the residual stress (σ^R_{re}) was obtained using Eq. (11). Considering the input residual stress (σ^R_{in}) as the nominal true value, we calculated errors for all cases (ε_y, n, and σ^R/σ_y were varied from 0.001 to 0.010, 0.05 to 0.30, and −0.9 to 0.9, respectively) as shown in Fig. 7. We found that the errors associated with the tensile residual stresses were lower than those associated with the compressive residual stresses and that smaller errors were associated with higher values of ε_y and n. In most cases, the maximum error was below 10% if $\sigma^R/\sigma_y > 0$ and below 20% if $\sigma^R/\sigma_y < 0$. Note that significant errors can occur if ε_y nears 0.001 and n nears 0.05.

3.3. Sensitivity analysis by error propagation

In experiments, errors are introduced when the loading curvatures are measured from indentations and when the properties of a material are obtained via tensile or indentation tests. These errors may lead to high variability in the estimation of residual stress. Therefore, it is necessary to investigate how sensitive the results obtained from the proposed method are to changes in $(c-c_0)/c_0$, ε_y, and n.

To characterize the sensitivity of the proposed method, we perturbed the values of $(c-c_0)/c_0$, ε_y, and n by 5%, 5%, and 0.02, respectively. After introducing these perturbations, the method depicted in Fig. 6 was adopted to evaluate the equi-biaxial residual stress (σ^R_{er}). The relative errors of the residual stress (i.e., $(\sigma^R_{er}-\sigma^R_{re})/\sigma^R_{re}$) were calculated and presented as three-dimensional maps (see Fig. 8). Fig. 8a and b show that for a 5% perturbation in ε_y, the maximum deviation of residual stress is approximately 17% with errors below 9% in most cases. Fig. 8c and d shows that for a 0.02 perturbation in n, the maximum deviation of residual stress is approximately 15% with errors that are usually below 4%. Because $(c-c_0)/c_0$ has a linear relationship with σ^R/σ_y, a 5% perturbation in $(c-c_0)/c_0$ leads to a 5% error in the residual stress estimation.

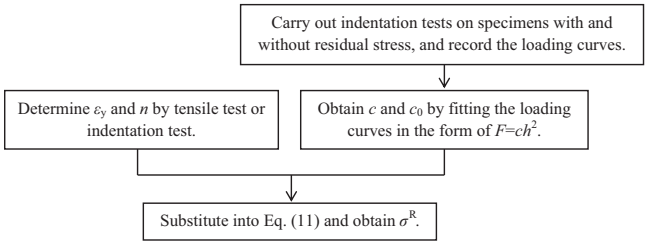

Fig. 6. A flow chart describing the methodology used for determining equi-biaxial residual stress with instrumented indentation.

3.4. Validity and reliability verification by experiment

Four commonly used metals (Al 2024, Al 7075, Copper C11000 and Ti Grade 5) were selected to verify the proposed method. These materials have a wide range of elasticities (see ε_y in Table 2).

To obtain the mechanical properties of these metals, we conducted uni-axial tensile tests at room temperature in accordance with ISO6892-1. For each type of material, three dumbbell-shaped specimens with rectangular cross-sections (10 mm × 3 mm) were processed. Using an extensometer (gauge length of 25 mm), the tests were performed on a MTS 810 material testing machine (MTS Systems Corporation, Eden Prairie, MN, USA) at a strain rate of 0.0023 s^{-1}. The elastic modulus (E), the yield stress (σ_y) and the strain-hardening exponent (n) were determined for each material (Table 2).

Instrumented sharp indentation tests were carried out to assess the validity of the proposed method. We designed a stress-applying apparatus, which could load the specimen with a well-defined external tensile/compressive force, to simulate the residual stresses inside the specimens (Fig. 9). A uniform uni-axial tensile stress (see Fig. 9a) could be applied to the specimen by screwing in the loading nut, while a uniform compressive stress (see Fig. 9b) could be applied by screwing in the loading bolt. Moreover, this load could be measured by the load cell, and the stress could be directly calculated (load divided by the cross-sectional area of the specimen (thickness approximately 3 mm, width approximately 4 mm)). In each experiment, the uni-axial pre-stress was kept below the elastic limit of each material. For each type of metal, five groups of stress states (two groups were tensile, two groups were compressive and one was stress-free) were applied. For each group, five indentation tests were performed using a universal hardness testing machine (ZHU2.5/Z2.5, Zwick/Roell Corporation, Ulm-Einsingen, Germany) equipped with a hardness measurement head and a Vickers indenter (see Fig. 9c). The work range of the built-in load cell varies from 5 to 2500 N with a force resolution of 0.01 N. The resolution of the displacement measurement is 0.02 μm. All of the indentation tests were conducted in load control mode using a three-step procedure that involved loading at a constant rate (1.7 N s^{-1}) to a prescribed maximum load (50 N), holding 10 s at the maximum load, and unloading using the same rate that was used during loading. The resulting mean loading curves were

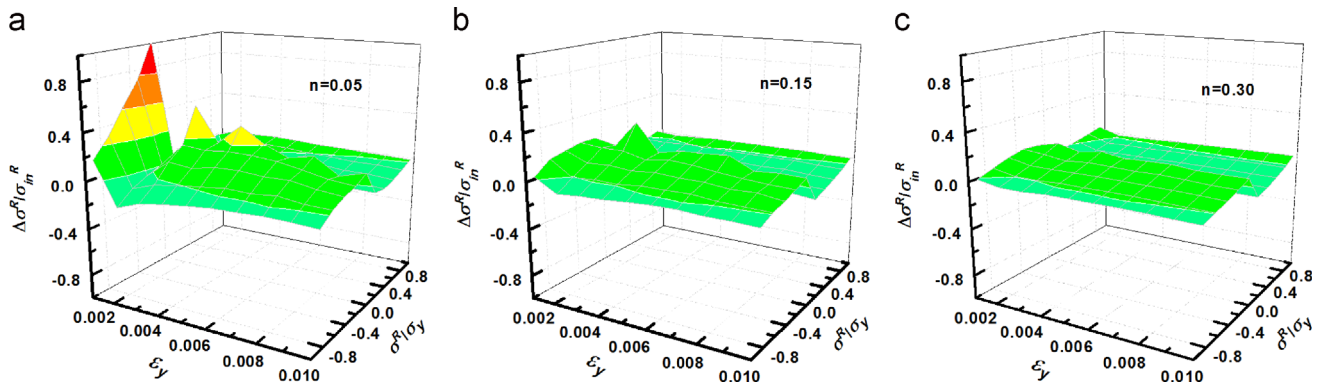

Fig. 7. Accuracy analysis of the reverse analysis for materials with varied ε_y and different n: (a) $n=0.05$; (b) $n=0.15$; (c) $n=0.30$. σ^R_{in} is the input residual stress value for the finite element analysis.

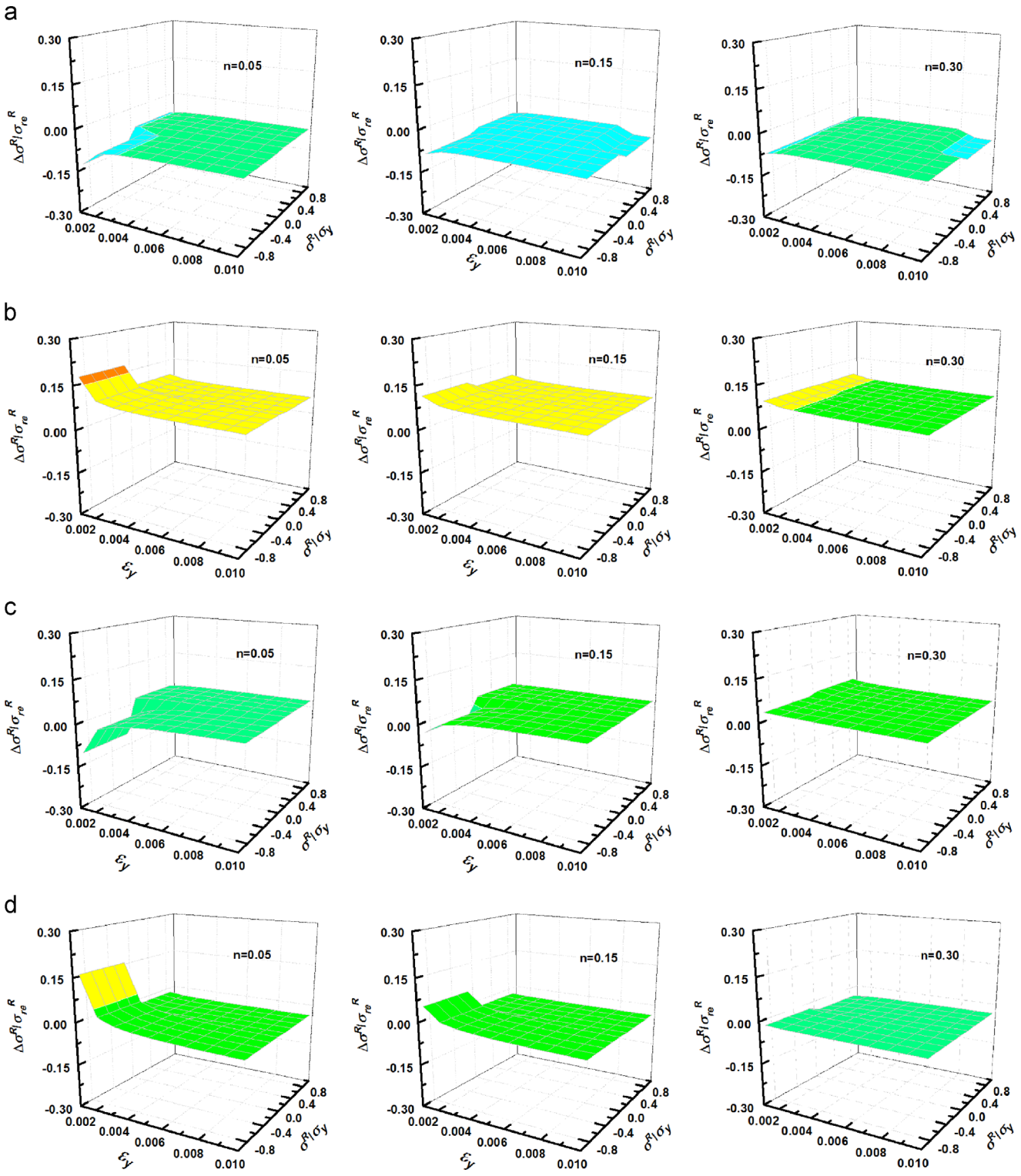

Fig. 8. Error sensitivity distribution of the residual stress estimation: (a) and (b) with +5% and −5% perturbations in ε_y; (c) and (d) with +0.02 and −0.02 perturbations in n. σ_{re}^R is the residual stress value obtained from the reverse analysis.

adopted (see Fig. 10) because there were minor differences in the loading curves obtained from each group when the same stress state was used. These data show that residual stress affects the indentation loading curves of these materials. In Fig. 10, the solid curves represent the behavior of the unstressed specimens. It is obvious that tensile residual stress tends to lower the loading curves, while compressive residual stress tends to raise the curves. By calculating the loading curvature for each curve, we could easily obtain the values of the stresses by substituting the calculated $(c-c_0)/c_0$ and the properties of the materials into Eq. (11). Because the half value of the uni-axial stress is equivalent to the equi-biaxial residual stress as Giannakopoulos [13] argued, the final values of the stresses (see Table 3) are twice the values we obtained using Eq. (11). The absolute errors between the nominal values measured using the load cell and the estimated values determined using the method proposed in the present work are commonly less than 50 MPa, and the relative errors are less than 20%.

Table 2
Materials' mechanical properties tested by uni-axial tensile tests.

Material	Elastic modulus E (GPa)		Yield stress σ_y (MPa)		$\varepsilon_y=\sigma_y/E$	Hardening exponent n	
	Mean $\overline{E}$	Std. ΔE	Mean $\overline{\sigma}_y$	Std. $\Delta\sigma_y$	Mean $\overline{\varepsilon}_y$	Mean $\overline{n}$	Std. Δn
Al 2024	71.4	0.4	350.8	2.5	0.0049	0.177	0.003
Al 7075	72.7	1.0	531.6	2.9	0.0073	0.107	0.002
Copper C11000	121.8	6.6	345.7	0.8	0.0028	0.016	0.002
Ti Grade 5	121.1	2.3	886.6	3.1	0.0073	0.057	0.002

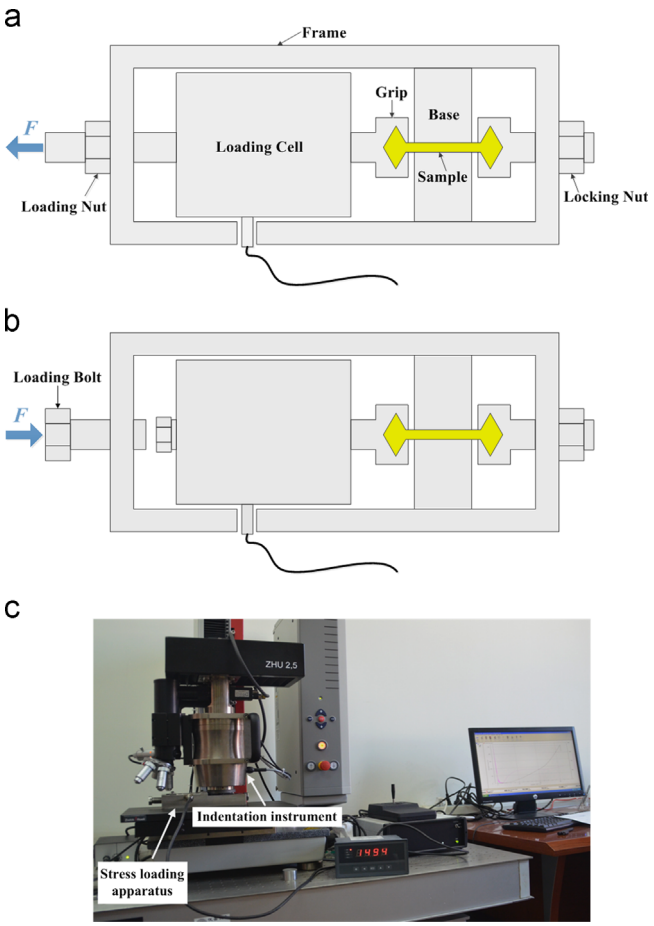

Fig. 9. A schematic of the uni-axial stress loading apparatus and testing machine: (a) loading apparatus for tensile stress; (b) loading apparatus for compressive stress; (c) the Zwick ZHU2.5/Z2.5 universal hardness testing machine.

3.5. *Validity and reliability verification using experimental data from the literature*

In addition, the proposed method was verified using experimental results found in the literature.

Lee et al. [8] performed sharp indentation tests on strained API X65 steel samples. In their experiments, all of the specimens were loaded to the same maximum indentation load. The authors did not provide the indentation curves in their paper, but gave the relative indentation depths at the maximum indentation loads. The absolute indentation depth for each average residual stress was calculated and listed in Table 4. The fractional change in loading curvature $((c-c_0)/c_0)$ can be approximated using

$$\frac{c-c_0}{c_0}\approx\left(\frac{h_0}{h}\right)^2-1, \tag{12}$$

where h and h_0 are the indentation depths at the same maximum indentation load with and without residual stress, respectively. As Sakharova et al. [4] mentioned, the elastic modulus (E), yield stress, and strain-hardening exponent of API X65 steel are 210 GPa, approximately 457 MPa, and approximately 0.1, respectively. By substituting the calculated values of $(c-c_0)/c_0$ and the properties of the material into Eq. (11), the residual stresses can be determined. Because Giannakopoulos [13] argued that the equi-biaxial residual stress is equivalent to the average residual stress, the final values of the stresses were twice those that we obtained using Eq. (11). As shown in Table 4, the estimated residual stresses are in good agreement with the nominal values from the literature.

Wang et al. [9] performed indentation tests on ion-implanted and unimplanted areas of a type of commercial stainless steel. The ion-implanted test induces a uniform equi-biaxial compressive residual stress. The loads with and without residual stress at the same indentation depth are 36 mN and 33 mN, respectively. The fractional change in loading curvature $((c-c_0)/c_0)$ can be approximated using

$$\frac{c-c_0}{c_0}\approx\frac{F-F_0}{F_0}, \tag{13}$$

where F and F_0 are the indentation loads at the same maximum indentation depth with and without residual stress, respectively. As Sakharova et al. [4] stated, the elastic modulus (E) of the material is 205 GPa, the yield stress is 1.04 GPa, and the strain-hardening exponent is approximately 0.3. By substituting the calculated value of $(c-c_0)/c_0$ and the material's properties into Eq. (11), the residual stress can be determined. The residual stress was calculated to be -612 MPa, which is close to the value that was reported by Wang et al. (-631 MPa).

4. Conclusion

A novel method that can be used to effectively estimate the surface equi-biaxial residual stress of a material has been proposed. This method does not require the contact area to be measured; it is often difficult to experimentally determine this value precisely. Instead, the fractional change in the loading curvature $((c-c_0)/c_0)$ was chosen as the analytical parameter, as it typically reflects the effect of residual stress on IIT outcomes and can be obtained much more precisely from the loading curves. A linear relationship between $(c-c_0)/c_0$ and σ^R/σ_y was found using dimensional and finite element analysis. The linear coefficient only depends on the mechanical parameters of the material. This linear relationship greatly simplifies the analytical expression that relates the residual stress to the indentation response. In addition, the proposed method was verified using four common metals, and a loading stress apparatus was designed. The resulting absolute errors between the estimated values determined using the proposed method and the nominal values measured using the load cell were typically less than 50 MPa, and the relative errors were less than 20%. Instrumented indentation data from the literature

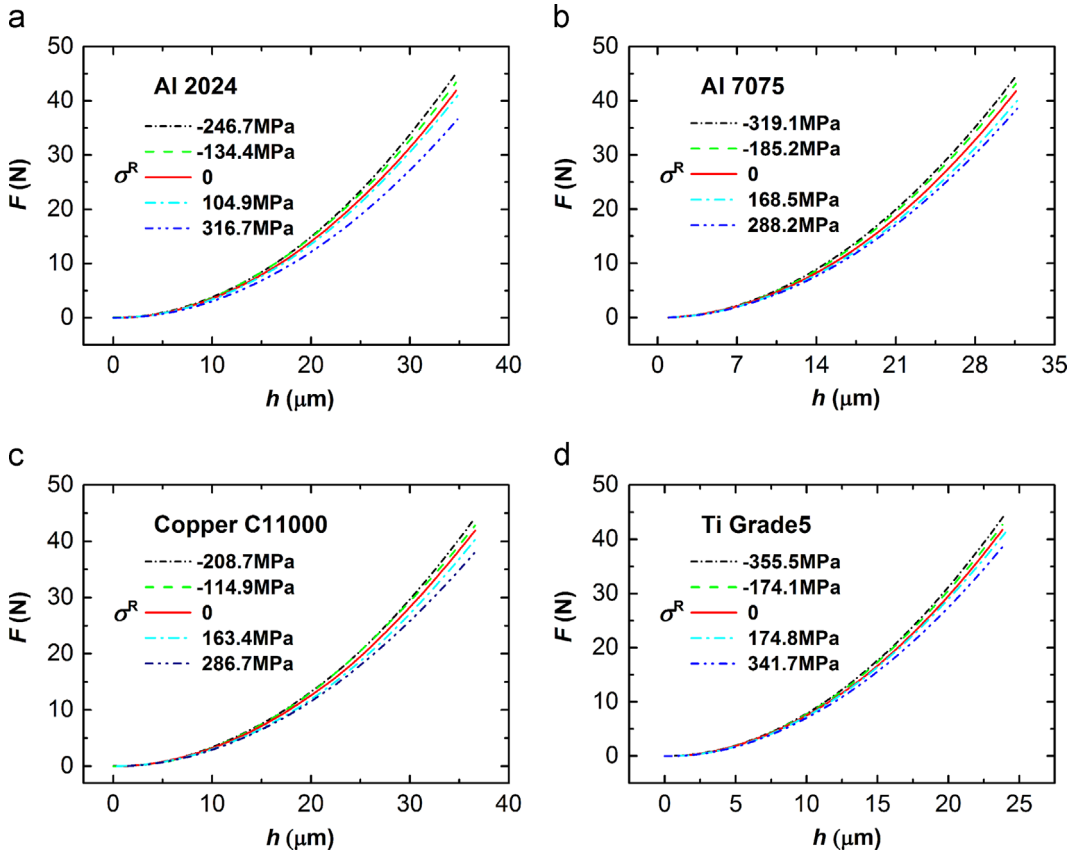

Fig. 10. The resulting mean loading curves of five indentations in each stress state for four metals: (a) Al 2024; (b) Al 7075; (c) Copper C11000; (d) Ti Grade 5.

Table 3
A comparison of the estimated stresses determined using the proposed method with the nominal stresses measured using a load cell. A nominal stress value of zero means that external forces are not applied in the group (which is treated as a reference).

Material	Nominal stress σ^R_{nor} (MPa)	Loading curvature c (GPa)	Estimated stress σ^R_{est} (MPa)	Absolute error $\sigma^R_{est}-\sigma^R_{nor}$ (MPa)	Relative error $(\sigma^R_{est}-\sigma^R_{nor})/\sigma^R_{nor}$ (%)
Al 2024	−246.7	37.516	−302.6	−55.9	22.7
	−134.4	36.285	−162.0	−27.6	20.5
	0	34.866	N.A.	N.A.	N.A.
	104.9	33.790	92.9	−12.0	−11.4
	316.7	30.157	406.4	89.7	28.3
Al 7075	−319.1	44.809	−341.2	−22.1	6.9
	−185.2	43.480	−188.1	−2.9	1.6
	0	41.841	N.A.	N.A.	N.A.
	168.5	39.836	175.8	7.3	4.3
	288.2	38.381	303.0	14.8	5.1
Copper C11000	−208.7	32.971	−249.2	−40.5	19.4
	−114.9	32.170	−128.0	−13.1	11.4
	0	31.323	N.A.	N.A.	N.A.
	163.4	30.033	118.1	−45.3	−27.7
	286.7	28.371	270.3	−16.4	−5.7
Ti Grade 5	−335.5	77.781	−420.8	−85.3	25.4
	−174.1	75.717	−208.9	−34.8	20.0
	0	73.683	N.A.	N.A.	N.A.
	174.8	71.762	147.4	−27.4	−15.7
	341.7	68.035	433.4	91.7	26.8

Table 4
A comparison of the estimated stresses determined using the proposed method with the nominal stresses from the literature.

Nominal stress σ^R_{nor} (MPa) [8]	Calculated indentation depth h (μm)	Estimated stress σ^R_{est} (MPa)	Relative error $(\sigma^R_{est}-\sigma^R_{nor})/\sigma^R_{nor}$ (%)
439.8	94.6	406.0	−7.7
282.6	91.6	275.0	−2.7
151.8	89.1	157.0	3.4
81.9	87.7	88.9	8.5

also confirmed that the estimated residual stress values determined by this method were in good agreement with the nominal values from the literature. Thus, we believe that the proposed method will be useful in the practical measurement of residual stress by instrumented indentation.

Acknowledgments

We acknowledge financial support from the National Natural Science Foundation of China (Nos. 11025212, 11272318, 11302231, 11172305, and 11372323).

References

[1] J. Lu, Handbook of Measurement of Residual Stresses, The Fairmont Press, Lilburn, Georgia, 1996.
[2] T.Y. Tsui, W.C. Oliver, G.M. Pharr, J. Mater. Res. 11 (1996) 752–759.
[3] A. Bolshakov, W.C. Oliver, G.M. Pharr, J. Mater. Res. 11 (1996) 760–768.
[4] N.A. Sakharova, P.A. Prates, M.C. Oliveira, J.V. Fernandes, J.M. Antunes, Strain 48 (2011) 75–87.
[5] S. Suresh, A.E. Giannakopoulos, Acta Mater. 46 (1998) 5755–5767.
[6] Y.-H. Lee, D. Kwon, Scr. Mater. 49 (2003) 459–465.
[7] M. Zhao, X. Chen, J. Yan, A.M. Karlsson, Acta Mater. 54 (2006) 2823–2832.
[8] Y.-H. Lee, K. Takashima, Y. Higo, D. Kwon, Scr. Mater. 51 (2004) 887–891.
[9] Q. Wang, K. Ozaki, H. Ishikawa, S. Nakano, H. Ogiso, Nucl. Instrum. Methods Phys. Res. 242 (2006) 88–92.
[10] P. Jiang, T.H. Zhang, Y.H. Feng, R. Yang, N.G. Liang, J. Mater. Res. 24 (2009) 1045–1053.
[11] ABAQUS, ABAQUS 6.11 User's Manual. Dassault Systèmes Simulia Inc., 2011.
[12] W.C. Oliver, G.M. Pharr, J. Mater. Res. 7 (1992) 1564–1583.
[13] A.E. Giannakopoulos, J. Appl. Mech. 70 (2003) 638–643.